*Article*

# Synthesis of Novel Tamarind Gum-co-Poly(Acrylamidoglycolic Acid) based pH Responsive semi-IPN Hydrogels and their Ag Nanocomposites for Controlled Release of Chemotherapeutics and Inactivation of Multi Drug Resistance Bacteria

**Kasula Nagaraja[1], Kummari S.V. Krishna Rao[1,] *, Sunmi Zo[2,3], Sung Soo Han[2,3], Kummara Madhususdana Rao[2,3,]***

[1] Polymer Biomaterial Design and Synthesis Laboratory, Department of Chemistry, Yogi Vemana University, Kadapa 516005, Andhra Pradesh, India; nagarajakasula33@gmail.com (K.N.)
[2] School of Chemical Engineering, Yeungnam University, 280 Daehak-Ro, Gyeongsan, Gyeongbuk, 38541, South of Korea;
[3] Research Institute of Cell Culture, Yeungnam University, 280 Daehak-Ro, Gyeongsan, Gyeongbuk 38541, South Korea sunmizo@ynu.ac.kr (S.Z.) ; sshan@yu.ac.kr (S.S.H.)
* Correspondence: ksvkr@yogivemanauniversity.ac.in; Tel: +919704278890 (K.S.V.K.R). msrao-chem@gmail.com (K.M.R.)

**Abstract:** Novel pH responsive semi-interpenetrating polymer hydrogels based on tamarind gum-co-poly(acrylamidoglycolic acid) (TMGA) polymers have been synthesized using simple free radical polymerization in the presence of bis[2-(methacryloyloxy)ethyl] phosphate as a crosslinker and potassium persulfate as a initiator. In addition, these hydrogels have been used as templates for green synthesis of silver nanoparticles (13.4±3.6 nm in diameter, TMGA-Ag) by using leaf extract of *Teminalia bellirica* as reducing agent. Swelling kinetics and equilibrium swelling behavior of the TMGA hydrogels have been investigated in various pH environment the maxium % equilibrium swelling behavior observed i.e., 2882±1.2. The synthesized hydrogels and silver nanocomposites have been characterized by the UV, FTIR, XRD, SEM and TEM. TMGA and TMGA-Ag hydrogels have been investigated to study the characteristics of drug delivery and antimicrobial study. Doxorubicin hydrochloride, a chemotherapeutic agent successfully encapsulated with maximum encapulstaion efficiency i.e., 69.20±1.2 and performed *in vitro* release studies in pH physiological and gastric environment at 37 °C. The drug release behavior is examined with kinetic models such as zero order, first order, Higuchi, Hixson Crowell, Korsmeyer-Peppas. These release data was the best fitted with the Korsemeyer-Peppas transport mechanism with n=0.91. Treatment effect on HCT116 Cell, human colon cancer cells were assessed with cell viability and cell cycle analysis. Antimicrobial activity of TMGA-Ag hydrogels is studied against to *Staphylococcus aureus* and *Klebsiella pneumonia*. Finally, the results demonstrate that TMGA and TMGA-Ag are promising candidates for anti-cancer drug delivery and inactivation of pathogenic bacteria, respectively.

**Keywords:** Tamarind Gum, Hydrogels, Semi-IPNs, Green synthesis, Silver Nanoparticles, Drug Delivery, Chemotherapeutics, HCT116 Cell, Anti-microbial.

## 1. Introduction

Functionalized interpenetrating polymer network (IPN) hydrogels have piqued the interest of researchers as potential materials in a wide range of medical and environmental applications, including affinity chromatography, immobilization technologies, drug-delivery systems, and organic dyes and heavy metal ion removal applications such as ion exchangers, adsorbents, and so on [1-6]. The importance of IPNs is growing due to the numerous opportunities for modifying their physico-chemical properties [7]. Natural polymers have successfully replaced a number of synthetic materials, either because the latter were in high cost or because the biodegradable and biocompatible properties of natural

Preprints (www.preprints.org) | NOT PEER-REVIEWED | Posted: 22 November 2021 doi:10.20944/preprints202111.0395.v1

polymers outperformed those of synthetic materials [8]. The success of natural polymer hydrogels as biomaterials is mostly owing to their resemblance to biological tissues and transformation processes, which allow them to be easily manufactured in a variety of forms and sizes at low manufacturing costs [9]. Natural polymers, on the other hand, have high biocompatibility but poor mechanical qualities; the necessity to preserve biological properties hampers their processing. Hence, to improve the physico-mechanical properties of the natural polymer-based hydrogels, they are blended, grafted and embedded with the compatible additives [9].

Recently, natural polymer based IPN type hydrogels are successfully developed for drug delivery, anti-microbial, wound healing, tissue engineering applications [7-9]. Banthia et al developed pH-sensitive polyacrylamide grafted pectin-based hydrogels for controlled release of salicylic acid. This salicylic drug release is observed at 86% within 7 h released. [10]. Krishna Rao et al developed pH and temperature responsive semi IPN hydrogel based on pectin and poly(2-dimethylamin)ethyl methacrylate for controlled drug delivery of 5-fluorouracil. These hydrogels were enhanced drug release in various stimuli responsive environments, finally, 100% drug release was observed within 80 h. These hydrogels could be used for the colon specific drug delivery applications [11]. Gautam Sen et al developed in sesbania gum based on hydrogel prepared by microwave assisted method using acrylamide as a monomer for sustained release applications of 5-flurouracil. These hydrogels enhanced to the drug release in alkaline medium [12]. Baljit sing et al developed poly(vinyl pyrrolidone) and *Azadirachta indica* gum based hydrogels for drug delivery of methyl prednisolone. These hydrogels enhanced drug release in phosphate buffer i.e., 45% prednisolone released in 24 h [13].

Tamarind gum (TMG) is one of the natural polysaccharides, it is a derivative of seeds of *Tamarindus indica linn,* which is widely available plant in India as well as Southeast Asia. TG consists of '(1-4)-β -D-glucan residues substituted with α-D-xylopyranose and β-D-galactopyranosyl (1-2)-α-D-xylopyranose linked (1-6) to glucose' moieties [14]. TMG is more pH tolerance as well as it shows the significant bioadhesive, due to this promising features, TMG-based materials have been used for drug delivery applications. pH responsive TMG polysaccharide and sodium alginate blend beads were developed for biotechnology applications [15]. Functionalized carbon nanotubes incorporated TMG hydrogels are developed for controlled release of tigecycline [16]. Graphene oxide based viscoelastic composite films were developed from the blends of poly(vinyl alcohol) and carboxy methyl TMG for controlled release of ciprofloxacin hydrochloride. Results of these films indicate that they have anti-microbial characteristics, which helps in human skin keratinocytes [17]. Floating beads are sodium alginate blended TMG with magnesium stearate were fabricated by ionotropic gelation technique for controlled release of risperidone [18]. Simvastatin based nanoparticles formulated from polyelectrolyte complexes of chitosan and TMG for anti-cancer applications [19].

Doxorubicin (DOX) is a commonly used chemotherapeutic drug used to treat a variety of cancers, including haematological malignancies and soft tissue sarcomas [20-23]. It is obtained from a *streptomyces species* and belongs to the anthracycline family, which has potential antibacterial and anticancer action[24,25]. It is an amphiphilic compound comprising a water insoluble aglycone and water-soluble amino sugar functional moiety. DOX's specific method of action is unknown, although it is thought to bind with DNA via intercalation and block topoisomerase. DOX's therapeutic applicability are limited due to numerous drug resistance and server-side effects. Furthermore, high dosages of DOX recommended to improve efficiency may have negative side effects on normal tissue cells, particularly those in the kidney and heart. Hence, to overcome the shortcomings of DOX, it was encapsulated or conjugated with polymeric systems [26-28].

In continuation of research work on natural polymer based functional materials for biomedical application [29] and based on the above facts, in this contribution, tamarind gum-co-poly(acrylamidoglycolic acid) based copolymeric semi-IPN hydrogels composed using bis[2-(methacryloyloxy)ethyl] phosphate as a potential crosslinker by simple free

 doi:10.20944/preprints202111.0395.v1

radical polymerization. These hydrogels are studied by FTIR, XRD, SEM, and TEM and are employed for *in vitro* controlled release of DOX, a chemotherapeutic drug. These hydrogels employed to study *in vitro* cell viability and cell cycle analysis of HCT116 Cell. Furthermore, these hydrogels were utilized in the green manufacture of silver nanocomposites employing aqueous leaf extract of *Teminalia bellirica*.

## 2. Results and Discussion

### *2.1. FTIR Spectroscopy studies*

Figure 1 shows the FTIR spectra of TMG polysaccharide, pure TMGA hydrogel, DOX, DOX loaded TMGA hydrogel, and TMGA-Ag. The pure tamarind gum (TMG) polysaccharide (Figure 1(A)) demonstrated a broad stretching vibration at 3416.32 $cm^{-1}$ for aliphatic -O-H and 2920.95 $cm^{-1}$ for -C-H groups. The pristine TMGA hydrogel spectrum is depicted in Figure 1(B), with peaks observed at 1729.52 $cm^{-1}$ and 1612.95 for (acid/amide) -C=O stretching vibration. The broad peak for TMG's -O-H bending vibration was recorded at 1380.95 $cm^{-1}$ [30-31]. Furthermore, peaks for P-O, P=O, and -C-O-C stretching vibrations emerged at 1216.19 and 1053 $cm^{-1}$, confirming the existence of phosphate crosslinker (BMEP). Figure 2 depicts the pure medication DOX is spectrum (C). DOX showed characteristic peaks at 3334.28 $cm^{-1}$, corresponding to -O-H and N-H stretching vibrations, and another peak at 1720 $cm^{-1}$, corresponding to -C=O stretching vibrations. The peak at 1592.38 $cm^{-1}$ corresponds to unsaturated -C=C- stretching vibration and 1399.04 $cm^{-1}$ corresponds to hydroxy group -O-H bending vibration. Figure 1(D) depicts the spectrum of a DOX-loaded TMGA hydrogel, with a characteristic peak at 3435.23 $cm^{-1}$ corresponding to the -O-H functional moiety and a peak at 1667 $cm^{-1}$ corresponding to the -CO-NH- functional moiety, and a peak at 1564 $cm^{-1}$ corresponding to the unsaturated -C=C- stretching vibration of DOX. Figure 1(E) shows the FTIR spectrum of a green synthesis of TMGA hydrogel silver nanocomposite using aqueous leaf extract *Terminali bellirica*; the stretching vibrational peaks 3425.12, 1612.89, 1389, and 1056.13 $cm^{-1}$ reveal the phenolic moiety, amide, and -C=O of hydrogels, respectively. The results show that TMG-based hydrogels can be successfully synthesized using simple free radical polymerization, DOX can be incorporated in TMGA hydrogels, and silver nanoparticles can be produced in an environmentally safe manner. Figure 2 depicts a probable schematic chemistry of TMGA hydrogel.

Preprints (www.preprints.org) | NOT PEER-REVIEWED | Posted: 22 November 2021 doi:10.20944/preprints202111.0395.v1

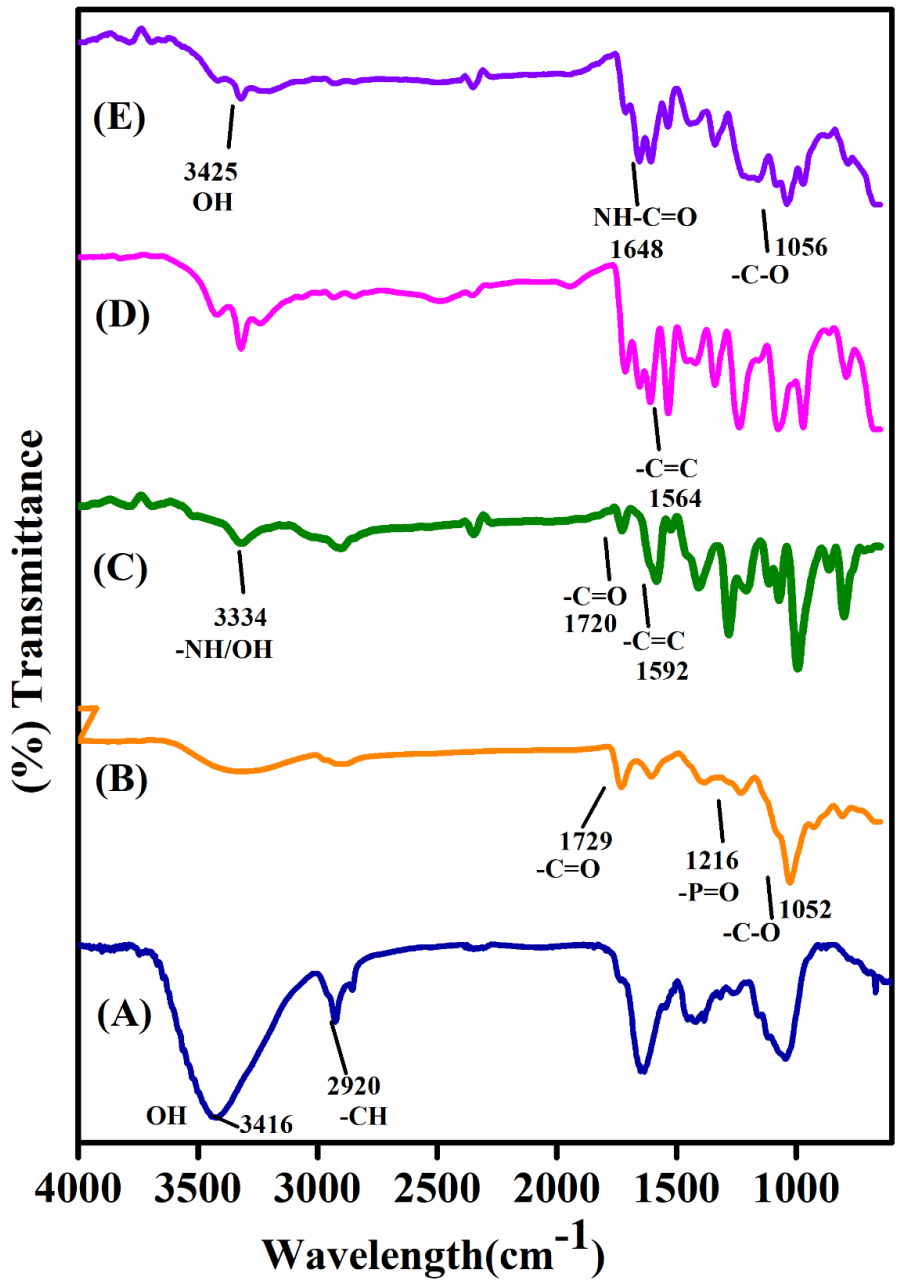


**Figure 1:** FTIR spectra of TMG polysaccharide (A), pristine TMGA hydrogel (B), DOX (C), DOX loaded TMGA hydrogel (D), TMGA-Ag (D).

Preprints (www.preprints.org) | NOT PEER-REVIEWED | Posted: 22 November 2021 doi:10.20944/preprints202111.0395.v1

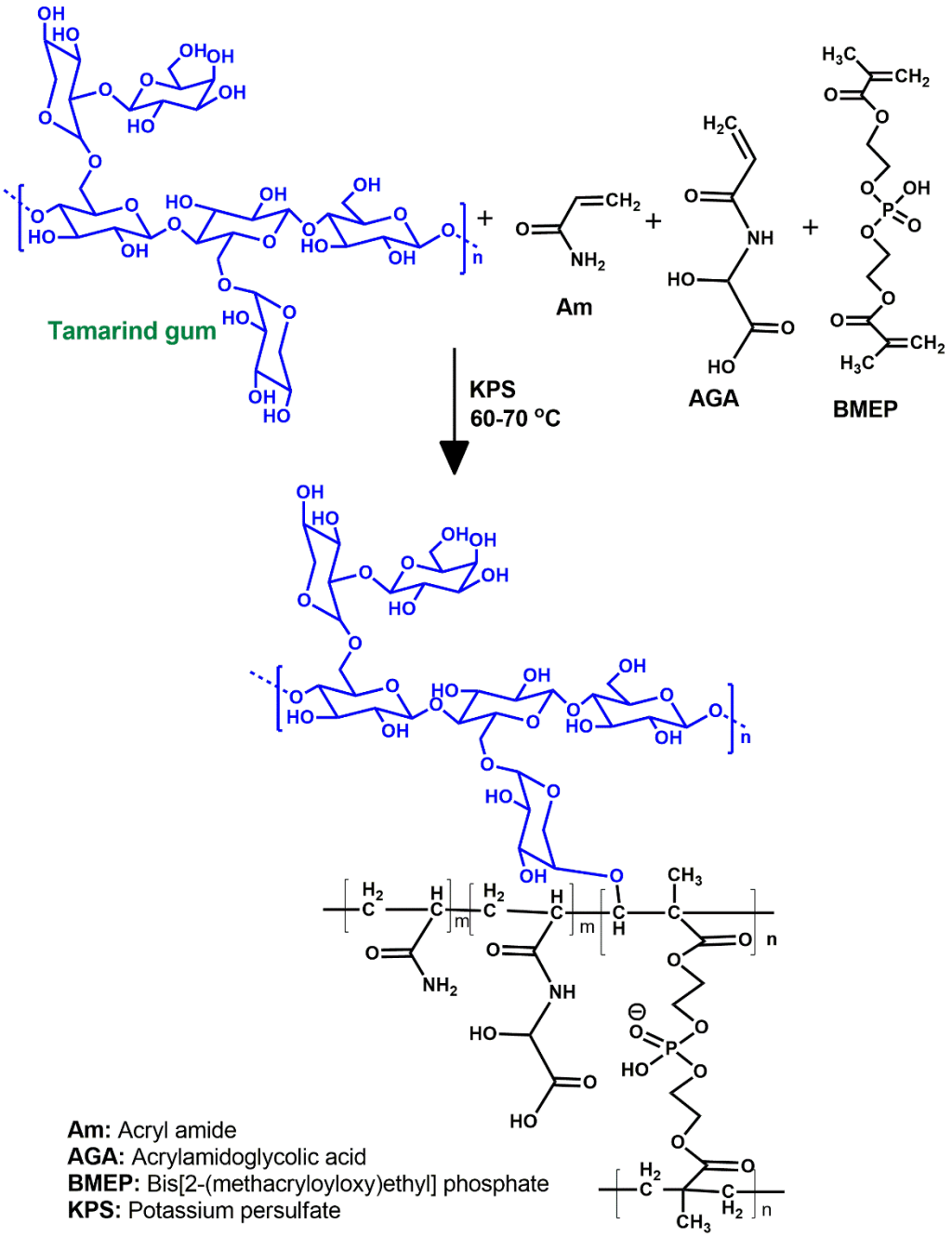


**Figure 2:** Plausible schematic chemistry of TMGA hydrogels

*2.2. UV-Visible spectroscopy*

TGM-derived natural polysaccharide-based hydrogels were employed as templates for the green synthesis of solver nanoparticles from *Terminalia bellirica* leaf extract, an eco-friendly reducing agent. Essentially, the reduction of silver ions to silver nanoparticles is proven by a colour change from light yellow to black at ambient temperature and a reaction time of 180 minutes, as shown in Figure 3. Significant absorption peaks are detected at 428-436 nm as a result of a quantum mechanical process known as surface plasmon resonance, which leads in the creation of silver nanoparticles within polymer networks with the help of polymer chains [32,33].

Preprints (www.preprints.org) | NOT PEER-REVIEWED | Posted: 22 November 2021 doi:10.20944/preprints202111.0395.v1

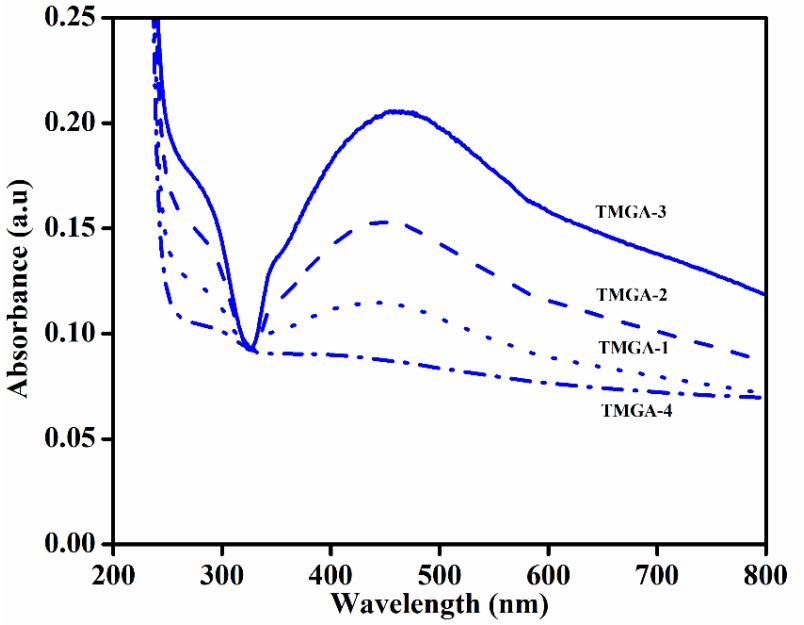


**Figure 3:** UV-Visible spectroscopy of TMGA-Ag hydrogels.

*2.3 X-Ray diffraction studies of TMGA hydrogel*

XRD was used to analyze the crystalline behavior of pure tamarind gum, pristine TMGA hydrogel, pure DOX, DOX loaded hydrogel, and TMGA-Ag hydrogel; the diffractograms are shown in Figure 4. The XRD curves of pure tamarind gum and pristine TMGA hydrogel (Figures 4A&B) are not shown any significant crystalline peaks, it may be due their amorphous behavior. However, the XRD curve of pure DOX (Figure 4.C) shows significant crystalline peaks at two theta values: 17.30°, 23.24°, 25.24°, 32.40°, 35.25°, and 40.29°. The DOX loaded TMGA hydrogel (Figure 4.D) showed characteristic DOX peaks at two theta values: 17.52°, 19.53°, 25.29°, showing that DOX is physically present, chemically stable, and molecularly distributed within the hydrogel network. The XRD pattern of the TMGA-Ag hydrogel (Figure 4.E) showed typical peaks at 38.46°, 44.41°, 63.12 °, and 76.46 ° for planes (111), (200), (220), and (311), respectively [32,33]. These findings suggest that the silver nanoparticles found in the hydrogel network are face-centered cubic crystals in nature.

Preprints (www.preprints.org) | NOT PEER-REVIEWED | Posted: 22 November 2021 doi:10.20944/preprints202111.0395.v1

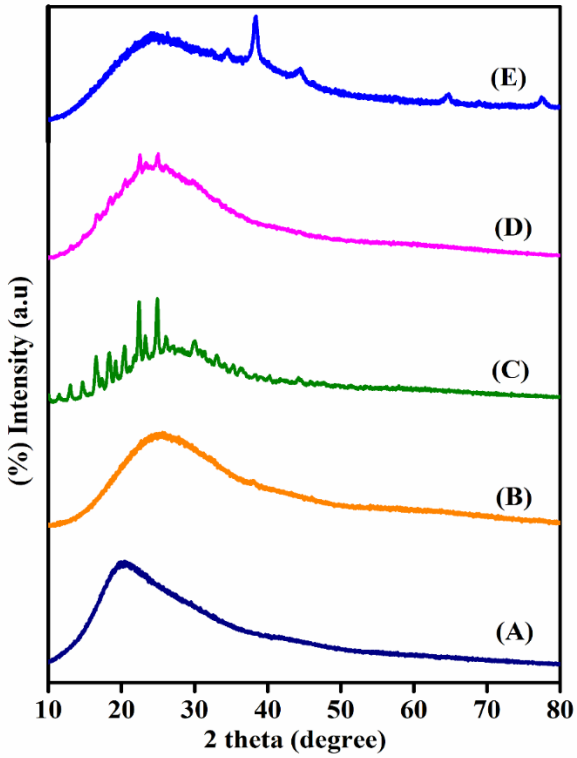


**Figure 4**: X-Ray diffraction spectra of TMGA hydrogel (A) Pure tamarind gum (B) Pristine TMGA hydrogel (C) Pure DOX (D) DOX loaded TMGA hydrogel (E) TMGA-Ag nanocomposites hydrogel.

*2.4. SEM and TEM studies*

SEM and TEM are most commonly employed technique for characterization of all types of materials to obtain quantitative data i.e., morphology and particle size. The surface morphology and elemental analysis were analyzed for pristine TMGA hydrogel, DOX loaded hydrogel, and TMGA-Ag hydrogels was examined with the SEM and TEM, images are shown in Figure 5. Pristine hydrogel exhibited the smooth surface owing to hydrophilic behavior of functional moieties (hydroxyl and amide) present in polymer network. (Fig. 5 (A & B) DOX loaded TMGA hydrogel has rough surface compared to pristine hydrogel (Figure 5 C) , it mey be due to (1) the presence of DOX molecules in and outside the network, which are formed as debris at the time of dehydration; (2) the surface have a high surface area based on the synthesis process, resulting in the rough surface The Ag nanoparticles have produced by a green method using aqueous leaf extract of to reduce the $Ag^{+}$ ions. Figure 5 D, E &F, shows the SEM and TEM images of PMGA-Ag hydrogel and Ag nanoparticles, respectively. TEM images ae evident that that Ag nanoparticles are mainly spherical shapes and formed without any aggregation. This suggests that, green synthesis of nanoparticles by green methods is good. Presence of silver element and size of Ag nanoparticles inner side of the hydrogel was examined with the energy-dispersive X-ray spectroscopy (EDX). The EDX spectrums Figure 5 G &H are before and after production of silver nanoparticles in TMGA hydrogels; TMGA-Ag hydrogel shown optical absorption peak were observed at 3.02 kV.

Preprints (www.preprints.org) | NOT PEER-REVIEWED | Posted: 22 November 2021 doi:10.20944/preprints202111.0395.v1

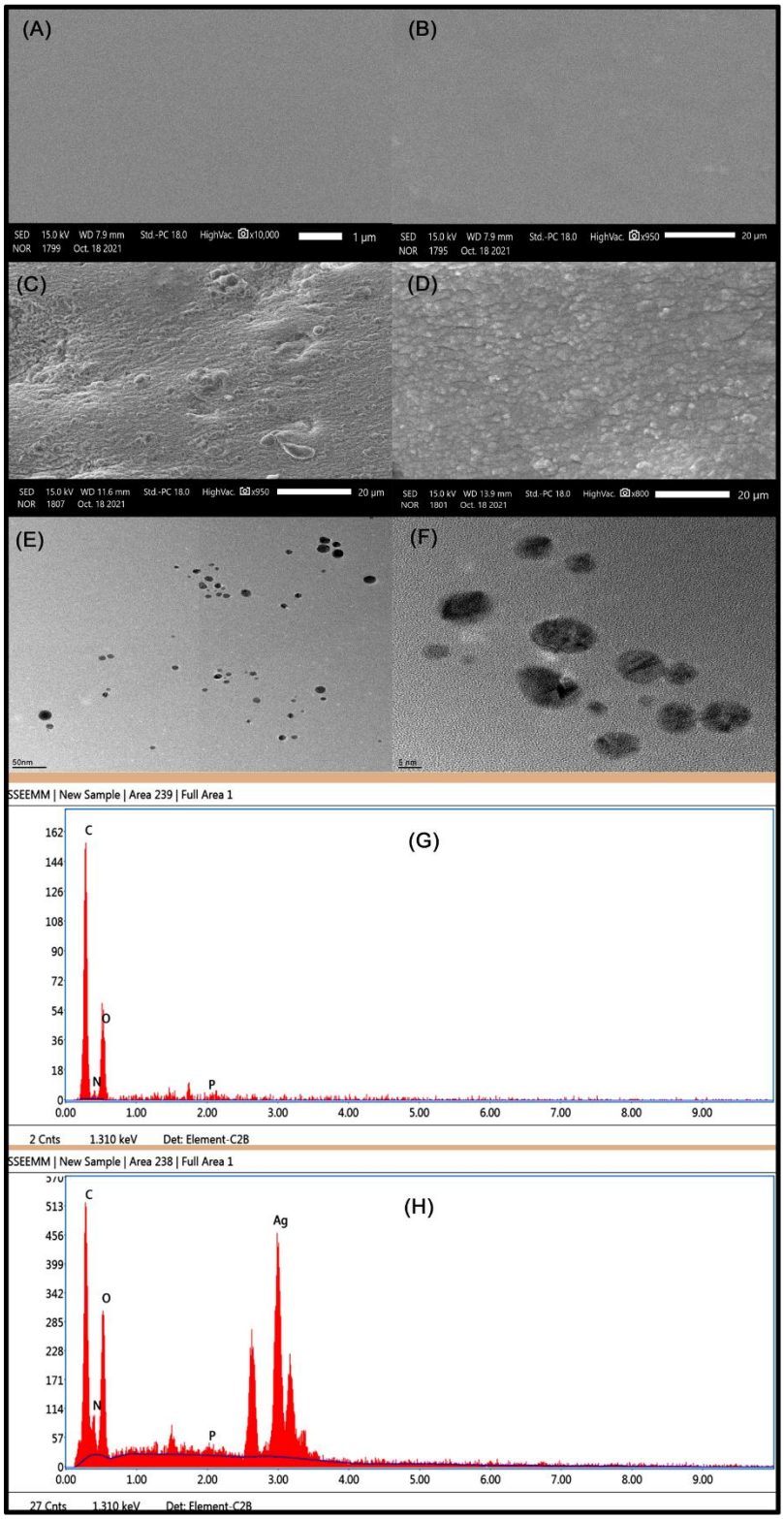


**Figure 5:** SEM and TEM images of TMGA hydrogels (A&B) Pure hydrogel (C) Drug composite hydrogel (D) TMGA-AgNPs hydrogel and (E&F) TEM images of AgNPs ((G) Dox loaded TMGA EDX spectrum (H) TMGA-AgNPs EDX spectrum.

*2.5. Swelling Studies*

 doi:10.20944/preprints202111.0395.v1

At room temperature, TMGA hydrogels were tested for (%) swelling ratio, (%) equilibrium swelling ratio (ESR), and pH-equilibrium swelling ratio (table 1). Figure 6 depicts the swelling kinetics of TMGA hydrogels as well as pH-dependent equilibrium swelling. Among the all-formulations examined for swelling studies, the TMGA-3 (2882) had the highest swelling ratio and the TMGA-4 (2040) had the lowest. The results show that the swelling ratio of TMGA hydrogels increases when AGA concentration increases and reduces as BMEP concentration increases. pH dependent equilibrium swelling experiments of TMGA hydrogels evaluated at various pH media (1, 3, 5, 7, 9 and 11). The presence of functional groups such as -OH and -COOH, which is associated to more ionizable hydroxy and carboxylate ions in a basic environment, may explain why the percent ESR was higher in the alkaline zone rather than the acidic.

For synthesized TMGA hydrogels, structural network parameters such as average molecular weight between crosslinkers (degree of crosslinking), polymer network volume fraction ($V_{2s}$), mesh size ($\xi$), polymer crosslinker density ($\upsilon_e$), and solvent interaction parameter of polymer network chain ($\chi$) were calculated using swelling results, and the results are shown in Table.1. With rising monomer (AGA) concentration and lowering crosslinker (BMEP) concentration, the average molecular weight between crosslinkers $M_c$ and $\xi$ values rose. The polymer solvent interaction values of prepared all hydrogels were approximately 0.52-0.54, indicating that the hydrogel network had good polymer solvent interactions. The data values for crosslinking density range from 0.11 to 0.54. These findings suggested that hydrogels get more hydrophilic as monomer content (AGA) increases, and that hydrogels become softer and have a stronger network [29,31].

Preprints (www.preprints.org) | NOT PEER-REVIEWED | Posted: 22 November 2021 doi:10.20944/preprints202111.0395.v1

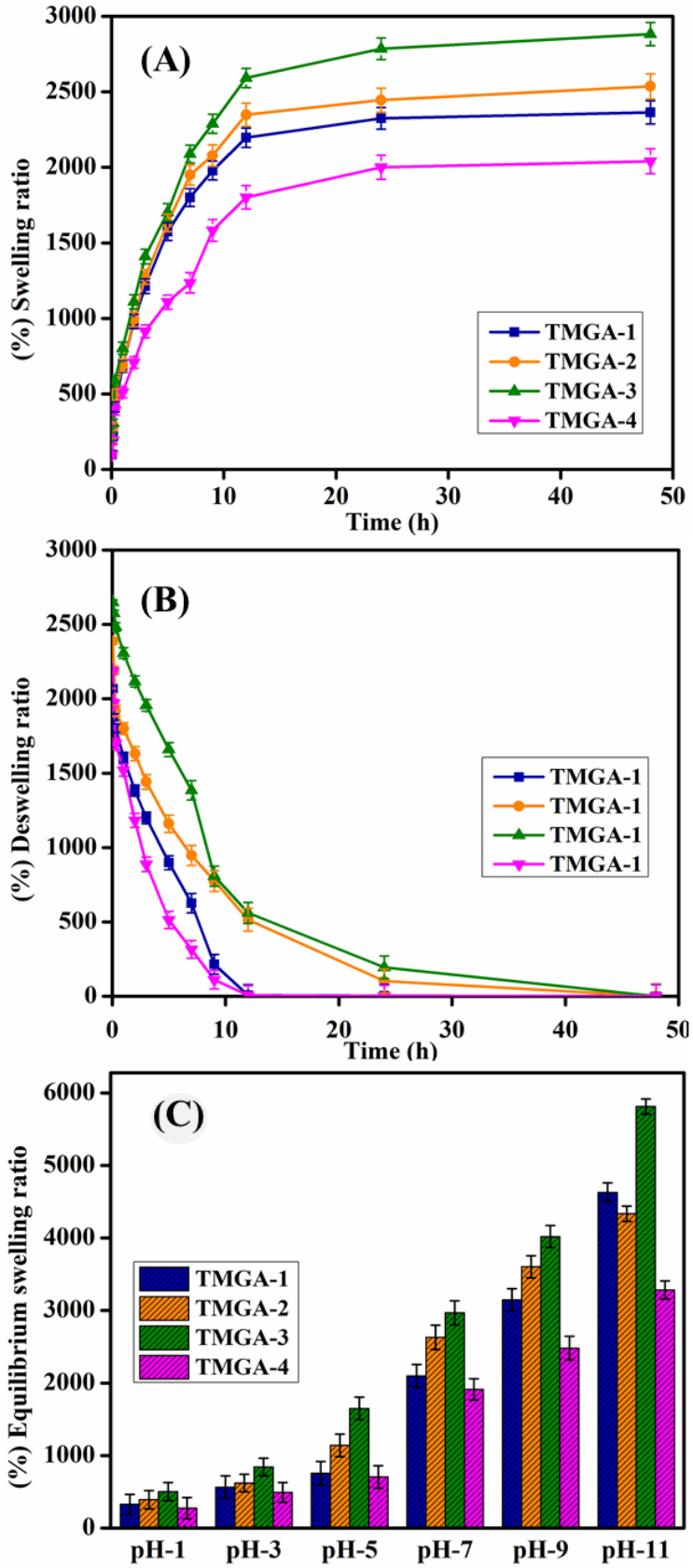


**Figure 6:** Swelling studies of TMGA hydrogels, (A) Swelling (B) Deswelling (C) pH-equilibrium swelling.

Preprints (www.preprints.org) | NOT PEER-REVIEWED | Posted: 22 November 2021 doi:10.20944/preprints202111.0395.v1

**Table 1.** Feed composition of TMGA hydrogel, %equilibrium swelling (%ESR), %encapsulation efficiency (%EE) and network parameters.

| Sample code | TMG (2%) (mL) | Am (g) | AGA (g) | BMEP (2 %) (w/v) (mL) | KPS 10% (w/v) (mL) | % ESR | % EE | Network parameters | | | | |
|---|---|---|---|---|---|---|---|---|---|---|---|---|
| | | | | | | | | χ | $M_c$ | ξ | ø | $\upsilon_e$ |
| **TMGA-1** | 5.0 | 0.5 | 0.5 | 2.0 | 1.0 | 2364±1.0 | 39.61±1.0 | 0.5456 | 29653 | 39.451 | 12.659 | 0.4552 |
| **TMGA-2** | 5.0 | 0.5 | 1.0 | 2.0 | 1.0 | 2536±0.7 | 56.56±0.8 | 0.5325 | 36039 | 50.125 | 11.478 | 0.1256 |
| **TMGA-3** | 5.0 | 0.5 | 1.5 | 1.0 | 1.0 | 2882±1.2 | 69.20±1.2 | 0.5238 | 61464 | 66.265 | 10.355 | 0.1125 |
| **TMGA-4** | 5.0 | 0.5 | 1.0 | 3.0 | 1.0 | 2040±0.9 | 31.86±1.3 | 0.5243 | 21782 | 32.236 | 15.119 | 0. 5426 |

*2.6. Encapsulation and in vitro DOX release of TMGA hydrogels:*

The percentage of DOX encapsulation efficiency data of TMGA hydrogel were shown in table 1; these values are ranged between 31.86 ± 1.3 to 69.20 ± 1.2, The maximum (%) EE observed TMGA-3 and minimum for TMGA-4; i.e., these values influenced by monomer and crosslinker in the hydrogel network. DOX-encapsulated TMGA hydrogels were tested using a tablet dissolution tester at 37 °Cin various buffer solutions such as pH -1.2 (simulated gastric region) and pH -7.4 (simulated intestinal region). DOX release kinetics shown against (percentage of total drug release vs. time). *In vitro* DOX release studies were performed in pH 7.4 & 1.2 at 25 & 37 ℃ release data is presented in the Fig. 7. DOX release results demonstrate that, drug is more release in pH 7.4 compare to pH 1.2. it may be due to the pH responsive -COOH group of PAGA polymer chains (data shown in Table S1). this may be because TMGA hydrogels contain more hydrophilic groups and easily ionizable functionalities, such as carboxylic (-COOH) acid and hydroxyl (-OH); thus, more ionization polymer network in phosphate buffer solution may be due to hydrogel expansion and ionic repulsion of $COO^-$ and -OH functionality, results in the formation of high release DOX from the hydrogel network [34-36]. This behaviour clearly observed for TMGA-3, as increasing concentration of monomer drug release is more and increasing concentration of crosslinker drug release is low. Further, these results are supported by the equilibrium swelling data.

Preprints (www.preprints.org) | NOT PEER-REVIEWED | Posted: 22 November 2021 doi:10.20944/preprints202111.0395.v1

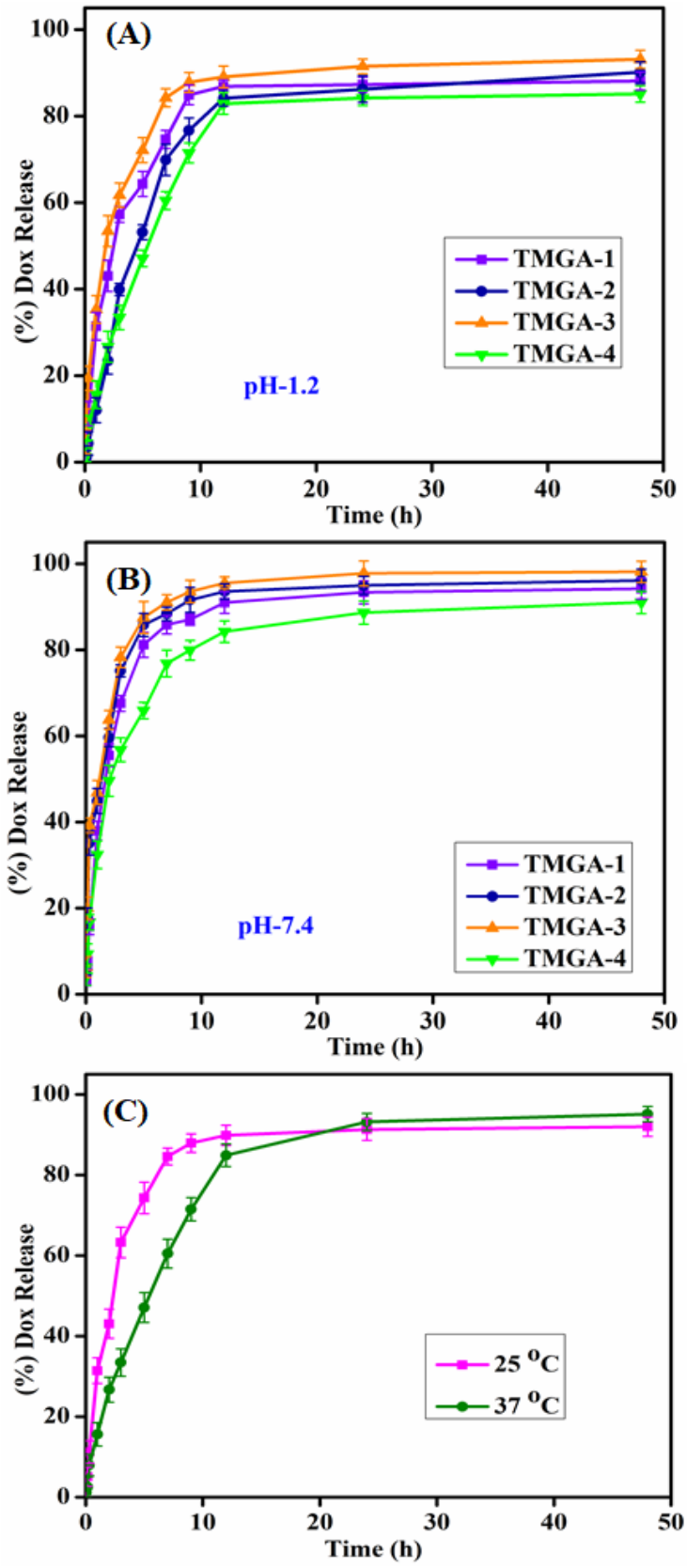


**Figure 7:** *In-vitro* DOX release studies ofTMGA hydrogel (A) pH-1.2 (B) pH-7.4, and (C) pH- 7.4 at 25 & 37 ℃.

Preprints (www.preprints.org) | NOT PEER-REVIEWED | Posted: 22 November 2021 doi:10.20944/preprints202111.0395.v1

DOX release data fitted with various kinetics models such as Higuchi square root, Hixson-Crowell cube root, zero order, first order, and Korsmeyer-Peppas equation, are shown in Table.S1. The *in vitro* drug release kinetics mechanism best fitted to Korsmeyer-peppas equation. The instance with a $n < 0.45$ polymer network following the Fickian diffusion, the second case between $0.45 < n < 0.89$ corresponds to the non-Fickian diffusion and anomalous mechanism, in third case n=1 totally non-Fickian and super case II drug release kinetics [22].

*2.7. Cell viability assay and cell cycle analysis of TMGA hydrogel*

Cancer cells of HCT-116 (Human colorectal adenocarcinoma) cell line was incubated different concentration (6.25, 12.5, 25, 50 and 100) of pure TMGA, DOX, and DOX loaded TMGA hydrogel cell viability investigated through MTT assay [Figure 8]. From the MTT assay, $IC_{50}$ values observed for pure TMGA hydrogel, pure DOX and DOX loaded TMGA 51.42 μg/mL, 6.67 μg/mL and 31.54 μg/mL, respectively. The pure TMGA hydrogel cell viability higher $IC_{50}$ values with lower cytotoxicity; DOX loaded TMGA hydrogel exhibited significant cytotoxicity, compare to hydrogel formulation free DOX is more toxic as it is obvious [37-39].

The cell cycle analysis was perused by staining treated and untreated cell line with PI and subsequently examined by flow cytometry. The percentage of distribution cells in different stages analysis for control and treated cells are presented in shown Figure 9. The cycle assay was report to used HCT-116 cells analyzed by pure TMGA hydrogel, free DOX, and DOX loaded TMGA hydrogel; apoptosis was investigated with flow cytometry. The untreated percentage of cell cycle were corresponding to sub G0/G1, 1.46%, G0/G1 79.65%, S phase 3.67% and G2/M 15.22, Pure TMGA hydrogel percentage of cell apoptosis given here sub G0/G1 1.43%, G0/G1 75.71%, S phase 35.11% and G2/M 17.39%, pure DOX percentage of cell apoptosis given data sub G0/G1 1.36%, G0/G1 57.2%, S phase 13.92% and G2/M 26.98%, DOX loaded TMGA hydrogel percentage of cell apoptosis given data sub G0/G1 2.93%, G0/G1 62.33%, S phase 12.13% and G2/M 21.68%, respectively; results indicate that the HCT116 cells under gone either apoptosis or necrosis.

Preprints (www.preprints.org) | NOT PEER-REVIEWED | Posted: 22 November 2021 doi:10.20944/preprints202111.0395.v1

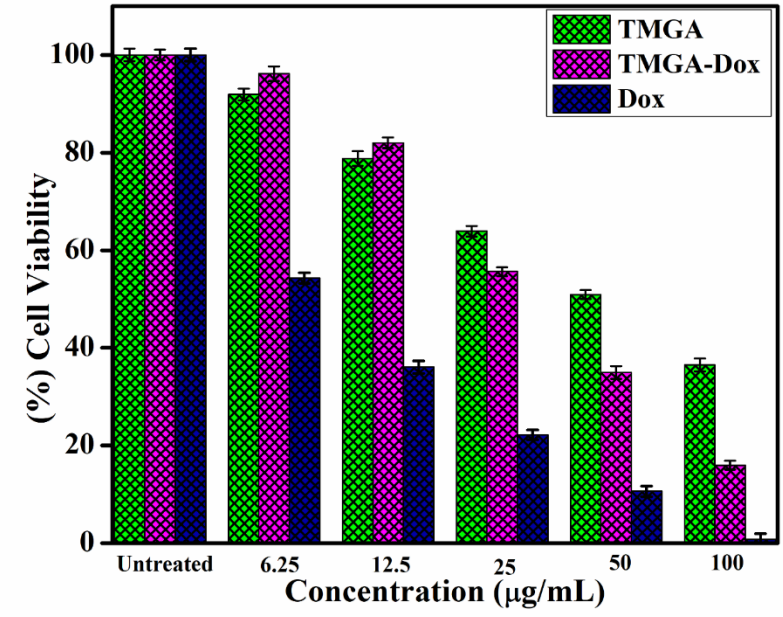


**Figure 8**: Cell viability studies of TMGA hydrogel, DOX, DOX loaded gel after 24 h incubation of HCT-116 cell lines.

Preprints (www.preprints.org) | NOT PEER-REVIEWED | Posted: 22 November 2021 doi:10.20944/preprints202111.0395.v1

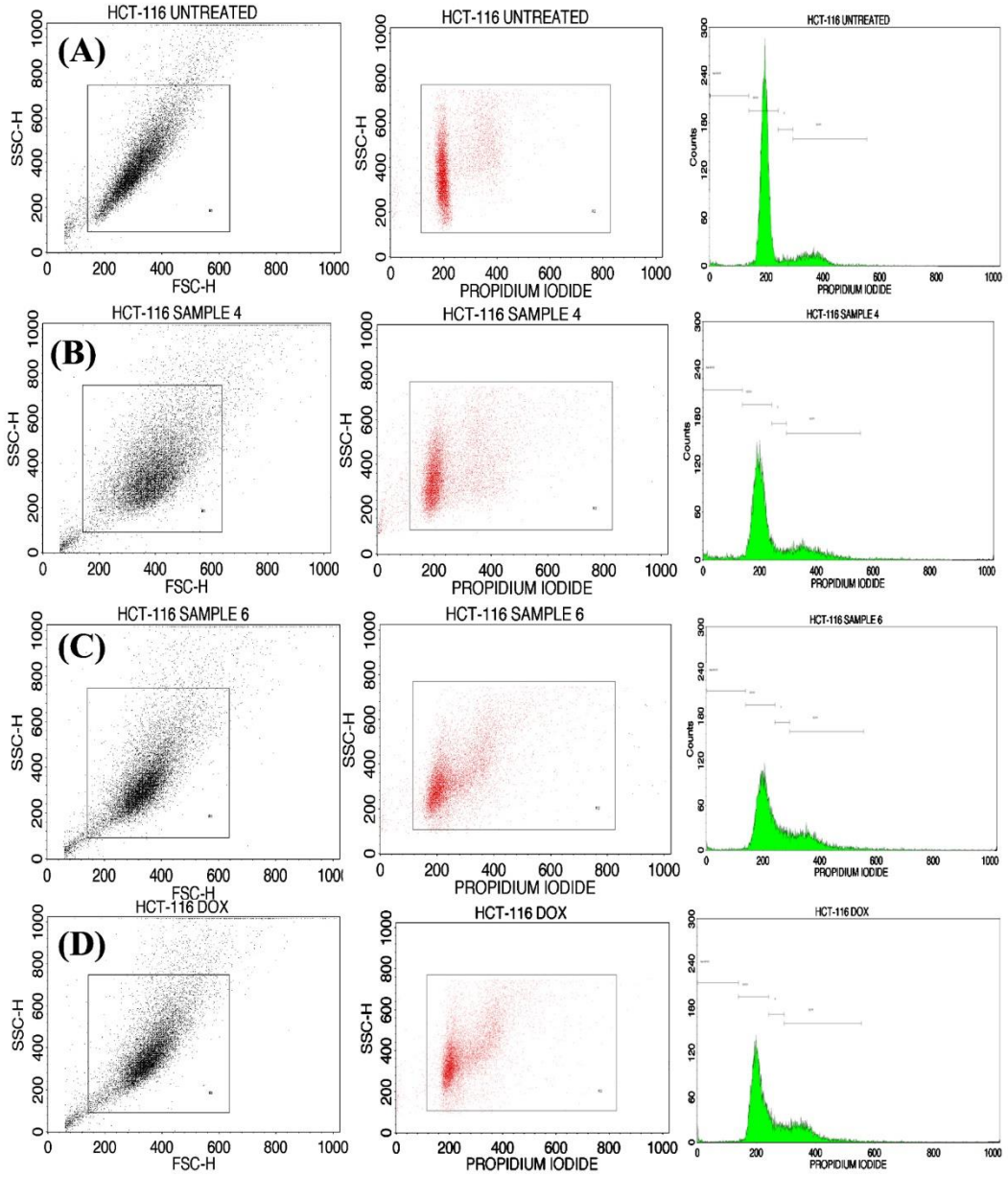


**Figure 9**: Cell cycle analysis of HCT116 cells (A) Untreated (B) TMGA hydrogel (C) Dox loaded TMGA hydrogel (D) Pure DOX.

*2.8. Anti-microbial Studies of TMGA-Ag nanocomposites*

The TMGA-Ag nanocomposite hydrogel was developed for the inactivation of multidrug resistance (MDR) bacteria, including both gram-positive and gram-negative bacteria [Figure 10]. Zone inhibition of TMGA-Ag against *Klebsiella pneumonia* was 6.0 mm, 9.0 mm, 6.0 mm, and 7.0 mm, and zone inhibition of *Staphylococcus aureus* was 4.0 mm, 7.0 mm, 8.0 mm, and 6.0 mm. The TMGA-Ags inhibited both gram and negative pathogen bacteria in the zone. The anionic nature of generated TMGA-Ags absorbed at the cell membrane's surface results in the formation of Ag nanoparticle diffusion, which leads to the inactivation of MDR bacteria [40,41].

Preprints (www.preprints.org) | NOT PEER-REVIEWED | Posted: 22 November 2021 doi:10.20944/preprints202111.0395.v1

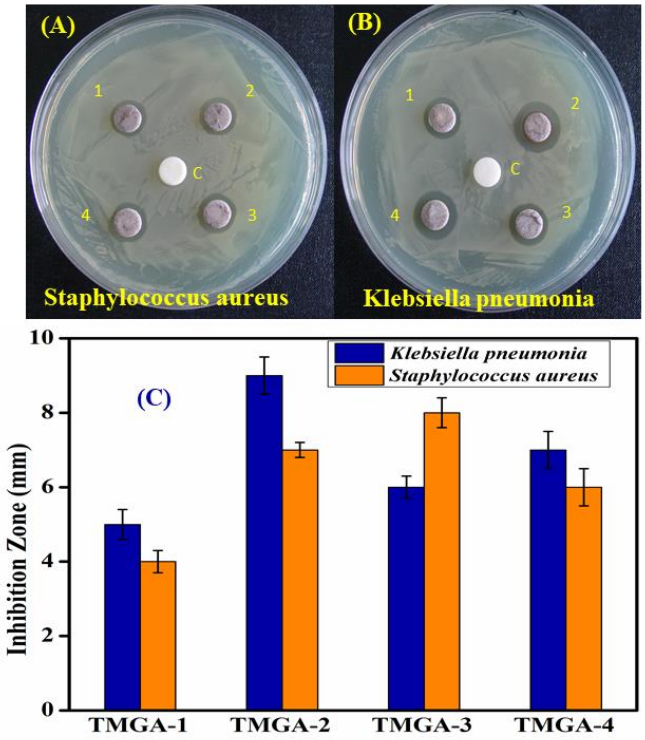


**Figure 10**: cell cycle analysis of HCT116 cells (A) Untreated (B) TMGA hydrogel (C) Dox loaded TMGA hydrogel (D) Pure DOX.

### 3. Conclusions

- In the current study, a simple free radical polymerization is used to synthesize an affordable, safe, biocompatible, and biodegradable tamarind gum polysaccharide and acylamidoglycolic acid based hydrogel (TMGA).
- TMGA hydrogels successfully utilized as templates for fabrication silver nanoparticles (13.4±3.6 nm in diameter) via green method using aqueous leaf extract of *Teminalia bellirica* as a reducing agent. TMGA-Ag nanocomposite hydrogel and identified with UV-visible absorption spectra $\lambda_{max}$ 425-432 nm.
- FT-IR, UV-Vis., XRD, SEM, EDS, and TEM were used to examine the chemical structure and functional groups of the pure TMGA hydrogel and TMGA-Ag nanocomposite hydrogels, as well as their morphological features of the hydrogel network.
- Doxorubicin hydrochloride (DOX) is encapsulated into the hydrogels with an encapsulation effectiveness i.e., 69.20±1.2 of DOX was successfully entrapped in the hydrogel network. After 48 hours in pH 7.4 at 37 $^{o}$C, the maximum percentage DOX release was 93.12 percent.
- *In vitro* DOX release of TMGA hydrogels was investigated using various kinetic models such as zero order, first order, Higuchi and Hixson-Crowell, and Korsmeyer-Peppas equations, as well as swelling kinetics, pH equilibrium, and network characteristics.
- The TMGA hydrogel totally followed the non-Fickian diffusion and was the best fitted with the model Korsemeyer-Peppas transport mechanism.
- The TMGA-Ag nanocomposites hydrogels efficiently inactivated MDR microorganisms *Staphylococcus aureus* and *Klebsiella pneumoniae*.
- Finally, the created hydrogel could be employed not only for pH triggered release of DOX but also any other hydrophilic chemotherapeutic agent and antibacterial applications based on the findings of this investigation.

Preprints (www.preprints.org) | NOT PEER-REVIEWED | Posted: 22 November 2021 doi:10.20944/preprints202111.0395.v1

## 4. Materials and Methods

### *4.1. Material and methods*

Bis(2-(methacryloyloxyethyl) phosphate (BMEP), acylamidoglycolic acid (AGA), and potassium persulphate (KPS) were purchased from Sigma-Aldrich (USA). Sodium hydroxide and hydrochloride were purchased from S.D Fine Chemical Limited (Mumbai, India). Acrylamide, silver nitrate and potassium dihydrogen phosphate ($KH_2PO_4$), were purchased from the Merck, Doxorubicin Hydrochloride (DOX) were received from the LC laboratories (MA, USA). Tamarind seeds were collected from the local market. Double distilled water (DDW) water was used for all experiments.

### *4.2. Isolation of tamarind gum (TMG) polysaccharide*

TMG is isolated as per the procedure published in elsewhere [14]. Briefly, the raw seeds of the tamarind fruit were collected and washed with DDW to remove the pulp and kernel, and 30 g of washed seeds were then crushed into small pieces and ground into a fine powder. The powder was taken in a 1000 mL glass beaker containing 600 mL water and boiled in water at both 60-70 °C. Constant stirring was maintained to attain viscous solution and the solution was filtered and washed twice with acetone and then with hexane. The precipitate was collected by centrifugation. The acetone and hexane were removed at 50 °C in a vacuum oven, and the filtrate TMG polysaccharide was stored in a refrigerator further used studies.

### *4.3. Synthesis of tamarind gum based hydrogels*

Aqueous TGM solution (2 % w/v) prepared and 5.0 mL solution was transferred to 50 mL beaker, to this, required quantities of acrylamide and acylamidoglycolic acid (AGA) monomers were added. Then, an initiator, potassium persulfate (1 mL 10 % aqueous solution) and a crosslinker, bis(2-(methacryloyloxy)ethyl phosphate (BMEP) (2.0 mL of 10 % aqueous solution) were added and stirred for 6 h to get homogenous solution. This reaction mixture was transferred to thermally controlled water bath (50 °C), with in 30 min reaction solution is converted in to transparent gel, however, the reaction continued for 4 h to make sure complete the reaction. The hydrogels formed (Figure S1) were then immersed in DDW to remove trace quantiles of unreacted chemical species and every 24 h changed water for 4 days. Finally, the hydrogels were dried at 40 °C in a hot air oven until a constant weight was reached.

### *4.4. Green synthesis of Ag-NPs hydrogel network*

300 mg of dried TMGA hydrogel weighed and was transferred into double distilled water. The swollen hydrogels were then transferred into 25 mL of $AgNO_3$ aqueous solution (5 mM) and then hydrogels were allowed to equilibrate for 30 h to ensure the maximum silver ions occupied inside in the hydrogel network. In this process, major amount of silver ions was exchanged from the solution into hydrogel network by hydrophilic groups of the hydrogel chain. The remaining metal ions occupied the free space of hydrogel network through ion-exchange process. These $Ag^+$ ions loaded hydrogel was transferred to another beaker containing 15 mL of aqueous leaf extract of *Teminalia bellirica*, results in the formation of the silver nanoparticles form silver ions within 2 h. The color of hydrogels was changed from light transparent to black, which confirms the formation of silver nanoparticles. The developed TMGA silver nanocomposite hydrogel (Figure S1) was washed in double distilled water then dried in a hot air oven at 40 °C.

### *4.5. Swelling studies of TMGA hydrogels*

TMGA hydrogel swelling kinetic studies were performed in double distilled water at 30 °C. The 100 mg of dried hydrogel taken in air-tight bottles containing 50 mL of double distilled water. The swollen hydrogel weight was measured after carefully wiping the surface-adhered water using a soft tissue paper. The equilibrium swelling was performed

Preprints (www.preprints.org) | NOT PEER-REVIEWED | Posted: 22 November 2021 doi:10.20944/preprints202111.0395.v1

in different pH solutions (1, 3, 5, 7, 9, and 11). The (%) swelling ratio (% SR) and (%) equilibrium swelling ratio (% ESR) were calculated based on the weights of the dried and swollen hydrogels using the following equation:

$$[\%]\ \text{Swelling ratio (SR)} = \left[\frac{w_s - w_d}{w_d}\right] \times 100 \quad (1)$$

$$[\%]\text{Equlibrium swelling ratio (ESR)} = \left[\frac{w_e - w_d}{w_d}\right] \times 100 \quad (2)$$

where, $m_s$, $m_d$, and $m_e$ are the swollen, dried, and equilibrium weights of the hydrogel, respectively.

*4.6. Network parameters of TMGA hydrogels*

TMGA hydrogel network parameters were calculated based on equilibrium-swelling data by using different equations [20]. The molecular mass between the crosslinks ($M_c$) calculated by following equation,

$$\bar{M}_c exp = -\left[\frac{(1-\frac{2}{\emptyset})v_1\rho_2(v_{2r})^{\frac{3}{2}}(v_{2m})^{\frac{1}{3}}}{\ln(1-v_{2m})+v_{2m}+\chi v_{2m}^{\ 2}}\right] \quad (3)$$

$$v_{2r} = \left[1 + \frac{\left[\frac{w_r}{w_d}-1\right]\rho_2-1}{\rho_1}\right] \quad (4)$$

$$v_{2m} = \left[1 + \frac{\left[\frac{w_s}{w_d}-1\right]\rho_2-1}{\rho_1}\right] \quad (5)$$

The Flory-Huggins interaction (polymer-solvent) parameter ($\chi$) was calculated as follows:

$$\chi = \frac{1}{2} + \frac{v_{2m}}{3} \quad (6)$$

The mesh size ($\xi$) and crosslinking density ($v_e$) network parameters was calculated as given follow equation,

$$\xi = 0.071\phi^{\frac{-1}{3}}(M_c)^{\frac{1}{2}} \quad (7)$$

$$v_e = \rho\sqrt{M_c} \quad (8)$$

*4.7. Drug loading and encapsulation efficiency*

The DOX, a chemotherapeutic agent was used as the model drug to examine the drug release characteristics of TMGA hydrogel. The DOX loading and encapsulation efficiency of TMGA hydrogel was done through the physical equilibrium swelling method. The dried TMGA hydrogel (about 200 mg) were transferred to 25 mL of DOX solution (1mg/mL), equilibrated the same for 24 h at room temperature, then removed the hydrogel and dried at 40 °C. The dried DOX loaded hydrogel 10 mg were placed into phosphate buffer solution (PBS) allowed for 48 h to come out the DOX completely. The residual DOX solution was analyzed through LAB INDIA ultra violet-visible spectrophotometer (model: UV-3092) at $\lambda_{max}$ 489 nm. The drug loading and encapsulation efficiency were calculated following equations [21].

$$[\%]\ \text{Drug loading} = \left[\frac{\text{Dox loaded TMGA hydrogel}}{\text{Amount of TMGA hydrogel}}\right] \times 100 \quad (9)$$

Preprints (www.preprints.org) | NOT PEER-REVIEWED | Posted: 22 November 2021 doi:10.20944/preprints202111.0395.v1

$$[\%]\ \mathrm{EE} = \left[\frac{\text{Actual loading of TMGA hydrogels}}{\text{Theoritical loading of TMGA hydrogel}}\right] \times 100 \quad (10)$$

*4.8. In-vitro drug release studies of TMGA hydrogels*

The TMGA drug loaded hydrogels was drug release carried out through tablet dissolution tester, thermo stated and consist of 8 basket LAB INDIA USP tablet dissolution tester (model: DS-8000). The dissolution rotation per speed 100 rpm constant, drug release rates were measured at 25 and 37°C. In-vitro drug release studies were performed by two different conditions such pH 1.2 (gastric region) and 7.4 (intestinal) phosphate buffer solutions. The baskets filled with 500 mL buffer solution and each sample dried drug loaded sample about 100 mg, regular time intervals; sample was taken out 5.0 mL subsequently and replaced with 5.0 mL fresh buffer solution. The amount of Dox released was analyzed through using Ultra violet visible spectrophotometer (LAB-INDIA, UV-3092) at fixed wavelength at 481 nm. The samples measurements were collected triplicate data estimation for standard deviation. The formulation TMGA-3 hydrogel experiments were also performed at 25 °C in pH 7.4 phosphate buffer solution.

*4.9. DOX Release Kinetic Parameters*

The results of DOX release studies of TMGA hydrogel were fitted with different kinetic release models, i.e., Higuchi square root, Hixson-Crowell cube root, zero order, first order, and Korsmeyer-Peppas equation were calculated the following equations [22].

$$M_t = K_h{}^{1/2}t \quad (11)$$

$$Q = Q_o - K_o t \quad (12)$$

$$lnQ = lnQ_o - K_1 t \quad (13)$$

$$Q^{1/3} = Q_0^{1/3} K_0 C \quad (14)$$

$$\frac{M_t}{M_\infty} = kt^n \quad (15)$$

where, where $m_t$: amount of drug released at time t, $K_h$: Higuchi rate constant, Q: amount of drug released at time t, $Q_0$: amount of drug released at time t=0; $K_1$: first order rate constant, $K_0$: zero-order rate constant, $K_C$: is the drug release constant Hixson-Crowell cube root law. $M_t$: drug release at time t, $M_\infty$: drug release at time ∞; and k: diffusion coefficient and n: diffusion exponent.

*4.10. Cell Viability and Cell cycle studies of TMGA-Ag hydrogels*

The cell viability of HCT-116 cell lines was tested using the MTT assay with pure TMGA hydrogel, DOX loaded hydrogel, and pure DOX. Flow Cytometry (BD Bioscience, San Jose, USA) was used to examine the HCT-116 cell cycle studies of pure TMGA hydrogel, DOX loaded hydrogel, and pure DOX. (1-2).

*4.11. Antimicrobial studies of TMGA-Ag hydrogels*

The TMGA-Ag hydrogel tested for antimicrobial activity of *Staphylococcus aureus* and *Klebsiella pneumonia* through the disk diffusion method [20]. The first nutrient agar media was prepared by mixing of peptone 5 g, beef extract 3 g and sodium chloride (NaCl) 5 g in double distilled water and pH of the mixture was adjusted to 7 and finally agar 15 g was added to the solution. Then agar medium was sterilized in autoclaved at pressure 15 lbs and temperature at 121 °Cfor 1h. This medium was transferred into petri dishes in laminar air flow chamber. An aqueous 4 mg/4 mL solution of the sample was prepared.

25 μL sample was then added to paper discs (6 mm) on the surface of the bacterial plates and incubated at 37 °Cfor 16 h. The zone of inhibition formed around the disc was measured.

*4.12. Characterization of TMGA-Ag hydrogels*

FTIR spectroscopy (Bruker Alpha-II, Eco-ATR) was performed to detect the various functional groups and chemical structures of the TMGA hydrogel network with scan range between 4000-600 $cm^{-1}$. The green synthesis of silver nanoparticles in hydrogel network was characterized by UV-visible spectroscopy (UV-vis, LAB INDIA, UV-3092) scan range between 200-800 nm. X-Ray diffraction (Rigaku, mini flex 600, JAPAN) of pure TMGA hydrogel and DOX loaded hydrogel was performed at a scanning speed 5o/min using Ni-filtered Cu-Kβ radiation range up to 10°-80° 2θ. The shape size and surface morphology studies of pure TMGA gel, DOX loaded TMGA hydrogel and its TMGA-Ag hydrogels were characterized by SEM (JEOL-IT500A, JAPAN) with acceleration voltages of 0.3 to 30kV. The sample were cut into about 20 mg hydrogel then coated with ultrafine gold coater and placed on the carbon stub acerated speed of voltage 0.2 to 30 kV. The morphology of TMGA hydrogel samples were studied using JEOL- IT500A, Made from JAPAN. The EDX (energy dispersive X-Rays) spectrum analysis of TMGA drug composite and TMGA-Ag nanocomposite hydrogel samples were analyzed by JEOL- IT500A, JAPAN.Ag-NPs embedded TMGA hydrogels was characterized by field emission transmission electron microscopy (TEM, FEI, Tecnai F20) operated 80 kV. The briefly colloidal aqueous TMGA-Ag nanocomposites hydrogel solution was casted on carbon coated 300 mesh copper grid and left for 30 min. The image was captured at different ranges magnification.

**Supplementary Materials:** $^{1}$H NMR of TMG polysaccharide (Figure S1) , Digital photograph of synthesized TMGA hydrogels (Figure S2), In-vitro drug release data of TMGA hydrogel (Table S1)and various drug release kinetic parameters (Table S2) are available online at www.mdpi.com/xxx/s1.

**Author Contributions:** Conceptualization, methodology, investigation, data curation, formal analysis, K.N.; Conceptualization, investigation, formal analysis, supervision, fund acquisition, writing-review and editing, K.S.V.K.R.; Fund acquisition, validation, formal analysis, S.Z; Fund acquisition, validation, formal analysis, S.S.H.; Fund acquisition, validation, formal analysis, writing-original draft preparation, K.M.R.

**Funding:** This research was supported by Basic Science Research Program through NRF of South Korea funded by Ministry of Education grant numbers: 2019R1I1A3A01063627; 2020R1A6A3A01100150/2020R1A6A1A03044512/2019R1I1A3A01063627

**Data Availability Statement:** Not applicable.

**Conflicts of Interest:** The authors declare no conflict of interest.

## References

1. Knipe, J.M.; Peppas, N.A. Multi-responsive hydrogels for drug delivery and tissue engineering applications. *Regenerative biomaterials* **2014**, *1(1)*, 57-65.
2. Wechsler, M.E.; Stephenson, R.E.; Murphy, A.C.; Oldenkamp, H.F.; Singh, A.; Peppas, N.A. Engineered microscale hydrogels for drug delivery, cell therapy, and sequencing. *Biomedical microdevices* **2019**, *21(2)*, 1-15.
3. Ahmad, H.; Nurunnabi, M.; Rahman, M.M.; Kumar, K.; Tauer, K.; Minami, H.; Gafur, M.A. Magnetically doped multi stimuli-responsive hydrogel microspheres with IPN structure and application in dye removal. *Colloids and Surfaces A: Physicochemical and Engineering Aspects* **2014,** *459*, 39-47.
4. Sivagangi Reddy, N.; Madhusudana Rao, K.; Sudha Vani, T.J.; Krishna Rao, K.S.V.; Lee, Y.I. Pectin/poly (acrylamide-co-acrylamidoglycolic acid) pH sensitive semi-IPN hydrogels: selective removal of Cu2+ and Ni2+, modeling, and kinetic studies. *Desalination and Water Treatment* **2016**, *57(14)*, 6503-6514.
5. Vani, T.S.; Reddy, N.S.; Reddy, P.R.; Rao, K.K.; Ramkumar, J.; Reddy, A.V.R. Synthesis, characterization, and metal uptake capacity of a new polyaniline and poly (acrylic acid) grafted sodium alginate/gelatin adsorbent. *Desalination and Water Treatment* **2014**, *52(1-3)*, 526-55.
6. Reddy, N.S.; Eswaramma, S.; Rao, K.K.; Reddy, A.V.R.; Ramkumar, J. Development of Hybrid Hydrogel Networks from Poly (Acrylamide-co-Acrylamido glycolic acid)/Cloisite Sodium for Adsorption of Methylene Blue. *Indian Journal of Advances in Chemical Science*, **2014**, *2*, 107-110.
7. Myung, D.; Waters, D.; Wiseman, M.; Duhamel, P.E.; Noolandi, J.; Ta, C.N.; Frank, C.W. Progress in the development of interpenetrating polymer network hydrogels. *Polymers for advanced technologies* **2008**, *19(6)*, 647-657.

8. Knipe, J.M.; Peppas, N.A. Multi-responsive hydrogels for drug delivery and tissue engineering applications. *Regenerative biomaterials* **2014**, *1(1)*, 57-65.
9. Reddy, N.S.; Rao, K.K.; Polymeric hydrogels: recent advances in toxic metal ion removal and anticancer drug delivery applications. *Indian Journal of Advances in Chemical Science*, **2016**, 4(2).
10. Sutar, P.B.; Mishra, R.K.; Pal, K.; Banthia, A.K. Development of pH sensitive polyacrylamide grafted pectin hydrogel for controlled drug delivery system. Journal of Materials Science: *Materials in Medicine* **2008**, *19(6)*, 2247-2253.
11. Eswaramma, S.; Reddy, N.S.; Rao, K.K. Phosphate crosslinked pectin based dual responsive hydrogel networks and nanocomposites: development, swelling dynamics and drug release characteristics. *International journal of biological macromolecules* **2017**, *103*, 1162-1172.
12. Pal, P.; Pandey, J.P; Sen, G. Sesbania gum based hydrogel as platform for sustained drug delivery: an 'in vitro'study of 5-Fu release. *International journal of biological macromolecules* **2018**, *113*, 1116-1124.
13. Singh, B.; Singh, B. Graft copolymerization of polyvinylpyrollidone onto Azadirachta indica gum polysaccharide in the presence of crosslinker to develop hydrogels for drug delivery applications. *International Journal of Biological Macromolecules* **2020**, *159*, 264-275.
14. Singh, R.; Malviya, R.; Sharma, P.K. Extraction and characterization of tamarind seed polysaccharide as a pharmaceutical excipient. *Pharmacognosy Journal* **2011**, *3(20)*, 17-19.
15. Zhang, J.; XU, S.; ZHANG, S.; Du, Z.; Preparation and characterization of tamarind gum/sodium alginate composite gel beads. *Iranian Polymer Journal* **2008**, *17 (12)*, 899-906.
16. Choudhary, B.; Paul, S.R.; Nayak, S.K.; Singh, V.K.; Anis, A.; Pal, K. Understanding the effect of functionalized carbon nanotubes on the properties of tamarind gum hydrogels. *Polymer Bulletin* **2018**, *75(11)*, 4929-4945.
17. Yadav, I.; Nayak, S.K.; Rathnam, V.S.; Banerjee, I.; Ray, S.S.; Anis, A.; Pal, K. Reinforcing effect of graphene oxide reinforcement on the properties of poly (vinyl alcohol) and carboxymethyl tamarind gum based phase-separated film. *Journal of the mechanical behavior of biomedical materials* **2018**, *81*, 61-71.
18. Bera, H.; Boddupalli, S.; Nandikonda, S.; Kumar, S.; Nayak, A.K. Alginate gel-coated oil-entrapped alginate–tamarind gum–magnesium stearate buoyant beads of risperidone. *International journal of biological macromolecules* **2015**, *78*, 102-111.
19. Malviya, R.; Raj, S.; Fuloria, S.; Subramaniyan, V.; Sathasivam, K.; Kumari, U.; Meenakshi, D.U.; Porwal, O.; Kumar, D.H.; Singh, A.; Chakravarthi, S. Evaluation of antitumor efficacy of chitosan-tamarind gum polysaccharide polyelectrolyte complex stabilized nanoparticles of simvastatin. *International journal of nanomedicine* **2021**., *16*, 2533.
20. Alle, M.; Kim, T.H.; Park, S.H.; Lee, S.H.; Kim, J.C. Doxorubicin-carboxymethyl xanthan gum capped gold nanoparticles: microwave synthesis, characterization, and anti-cancer activity. *Carbohydrate Polymers*, **2020**, *229*, 115511.
21. Mei, L.; Xu, K.; Zhai, Z.; He, S.; Zhu, T.; Zhong, W. Doxorubicin-reinforced supramolecular hydrogels of RGD-derived peptide conjugates for pH-responsive drug delivery. *Organic & Biomolecular Chemistry* **2019**, *17*(15), 3853-3860.
22. Kuddushi, M.; Ray, D.; Aswal, V.; Hoskins, C.; Malek, N. Poly (vinyl alcohol) and functionalized ionic liquid-based smart hydrogels for doxorubicin release. *ACS Applied Bio Materials*, **2020**, *3(8)*, 4883-4894.
23. Rao, K.K.; Zhong, Q.; Bielski, E.R.; da Rocha, S.R. Nanoparticles of pH-responsive, PEG–doxorubicin conjugates: Interaction with an in vitro model of lung adenocarcinoma and their direct formulation in propellant-based portable inhalers. *Molecular Pharmaceutics*, **2017**, *14*(11), 3866-3878.
24. Malla, S., Niraula, N.P., Liou, K. and Sohng, J.K., 2010. Self-resistance mechanism in Streptomyces peucetius: overexpression of drrA, drrB and drrC for doxorubicin enhancement. *Microbiological Research*, **2010**, *165(4)*, 259-267.
25. Naba, N.M.; Tolay, N.; ERMAN, M.B.; Yazgan, A.S. Doxorubicin inhibits miR-140 expression and upregulates PD-L1 expression in HCT116 cells, opposite to its effects on MDA-MB-231 cells. *Turkish Journal of Biology*, **2020**, *44*(1), 15-23.
26. Sun, Z.; Song, C.; Wang, C.; Hu, Y.; Wu, J. Hydrogel-based controlled drug delivery for cancer treatment: a review. *Molecular pharmaceutics* **2019**, *17*(2), 373-391.
27. Reddy, N.S.; Vijitha, R.; Rao, K.S.V.K. Polymer electrolyte membranes for fuel cell and drug delivery applications. In *Advances in Chemical Science & Biotechnology for Water Purification, Energy Production and Stress Management* KROS Publications India, **2021**, *1*, 95-134.
28. Rao, K.M.; Rao, K.S.V.K.; Ha, C.S. Functional stimuli-responsive polymeric network nanogels as cargo systems for targeted drug delivery and gene delivery in cancer cells. In *Design of Nanostructures for Theranostics Applications* William Andrew Publishing. **2018**, 243-275.
29. Nagaraja, K.; Rao, K.M.; Reddy, G.V; Rao, K.K.; Tragacanth gum-based multifunctional hydrogels and green synthesis of their silver nanocomposites for drug delivery and inactivation of multidrug resistant bacteria. *International Journal of Biological Macromolecules* **2021**, *174*, 502-511.
30. Tian, C.; Xu, P.; Jiang, J.; Han, C.; Preparation and drug-delivery study of functionalized hydroxyapatite based on natural polysaccharide gums with excellent drug-loading properties. *Journal of Dispersion Science and Technology* **2021**, *42*(5), 751-759.
31. Eswaramma, S.; Rao, K.S.V.K.; Rao, K.M. Diffusion and controlled release characteristics of pH-sensitive poly (2-(dimethyl amino) ethyl methacrylate-co-2-hydroxyethylacrylate) hydrogels. *International Journal of Polymeric Materials and Polymeric Biomaterials*, **2016**, *65*(3), 134-142.
32. Rao, K.S.V.K., Reddy, P.R., Rao, K.M. and Kumar, S.P. A green approach to synthesize silver nanoparticles from natural polymer for biomedical application. *Indian Journal of Advances in Chemical Science* **2015**, *3*, .340-344.
33. Espenti, C.S.; Rao, K.S.V.K.; Ramesh, P.; Sekhar, A.C.; Rao, K.M. Salacia mulbarica leaf extract mediated synthesis of silver nanoparticles for antibacterial and ct-DNA damage via releasing of reactive oxygen species. *IET nanobiotechnology*, **2020**, *14*(6), 485-490.
34. Eswaramma, S.; Rao, K.K. Synthesis of dual responsive carbohydrate polymer based IPN microbeads for controlled release of anti-HIV drug. *Carbohydrate Polymers* **2017**, *156*, 125-134.
35. Siepmann, J.; Kranz, H.; Bodmeier, R.; Peppas, N.A. HPMC-matrices for controlled drug delivery: a new model combining diffusion, swelling, and dissolution mechanisms and predicting the release kinetics. *Pharmaceutical research* **1999**, 16(11), 1748-1756.
36. Ma, Z., Ma, R., Wang, X., Gao, J., Zheng, Y., & Sun, Z. Enzyme and PH responsive 5-flurouracil (5-FU) loaded hydrogels based on olsalazine derivatives for colon-specific drug delivery. *European Polymer Journal* **2019** *118*, 64-70.

37. Liang, Y., Zhao, X., Ma, P. X., Guo, B., Du, Y., & Han, X. pH-responsive injectable hydrogels with mucosal adhesiveness based on chitosan-grafted-dihydrocaffeic acid and oxidized pullulan for localized drug delivery. *Journal of colloid and interface science*, **2019** *536*, 224-234.
38. Lee, Y., Arai, Y., Ahn, J., Kim, D., Oh, S., Kang, D., Lee, S. H. Three-dimensional microenvironmental priming of human mesenchymal stem cells in hydrogels facilitates efficient and rapid retroviral gene transduction via accelerated cell cycle synchronization. *NPG Asia Materials*, **2019** *11(1)*, 1-11.
39. Pérez, E., Fernández, A., Olmo, R., Teijón, J. M., & Blanco, M. D. pH and glutathion-responsive hydrogel for localized delivery of paclitaxel. *Colloids and Surfaces B: Biointerfaces* **2014** *116*, 247-256.
40. Liu, W., Li, X., Wong, Y. S., Zheng, W., Zhang, Y., Cao, W., & Chen, T. Selenium nanoparticles as a carrier of 5-fluorouracil to achieve anticancer synergism. *ACS nano* **2012** *6(8)*, 6578-6591.
41. Matai, I., Sachdev, A., & Gopinath, P. Multicomponent 5-fluorouracil loaded PAMAM stabilized-silver nanocomposites synergistically induce apoptosis in human cancer cells. *Biomaterial's science* **2015** *3(3)*, 457-468.